DIRECTION OF ARRIVAL ESTIMATION IN MIMO RADAR SYSTEMS WITH NONLINEAR REFLECTORS

Gal Shulkind, Gregory W. Wornell[*]

Department of EECS
Massachusetts Institute of Technology
Cambridge, MA, USA
{shulkind,gww}@mit.edu

Yuval Kochman[†]

Department of CSE
The Hebrew University of Jerusalem
Jerusalem, Israel
yuvalko@cs.huji.ac.il

ABSTRACT

Multiple-input multiple-output (MIMO) radar systems have been shown to offer superior performance in direction of arrival (DOA) estimation applications compared to their phased array counterparts. The performance of these systems has been studied under various probing field-target interaction mechanisms. However, to the best of our knowledge, these have been restricted to linearized models.
Motivated by various nonlinear imaging modalities we study DOA estimation in far field MIMO radar systems in conjunction with a power-law nonlinear probing field-target interaction mechanism and show that the nonlinearity increases the number of identifiable targets with a given number of antenna array elements.

Index Terms— MIMO radar, Nonlinear reflectance, Array design.

1. INTRODUCTION

Conventional phased array radar systems limit the number of degrees of freedom associated with the signal set by only allowing correlated transmission from different antenna elements. MIMO systems, which have been the focus of research over the last decade, allow transmission of uncorrelated signals. Stoica et al. [1] explored MIMO radar with co-located antennas. They considered configurations with N_t transmitting and N_r receiving antennas in conjunction with suitable signal sets and array configurations and have shown that in several respects performance gains may be attained compared to their conventional phased array counterparts. Specifically in terms of the number of identifiable targets the performance of a MIMO system with N_t transmit and N_r receive elements is comparable to that of a conventional system employing order $O(N_t N_r)$ elements. Other studies [2] have explored MIMO radar systems with distant antennas in conjunction with targets exhibiting reflection fluctuations and have shown that spatial diversity may be utilized to overcome deep fading conditions.
While various deterministic and stochastic probing field-target interaction models have been considered in the past, to the best of our knowledge all such studies have assumed a linearized response where the reflected field scales with the probing field.
In practice the interaction mechanism between the probing field and a distant scene may exhibit more complicated characteristics. As a motivating example, in recent years the use of micro-bubbles as a nonlinear contrast agent in medical ultrasound applications has become wide-spread [3]. The highly nonlinear interaction manifests itself in the reflected signal as harmonics of the incoming signal. Similar nonlinear phenomena have been utilized in conjunction with electromagnetic reflections in microscopy applications [4].
In this work we consider the consequences of a hypothetical memoryless, *k*th order power-law nonlinear target reflectance model on the design and performance of MIMO radar systems used in DOA estimation applications. We show that in conjunction with a specialized probing signal set and array design a MIMO radar system with N_t transmit and N_r receive elements can attain target identification performance comparable to that of an $O(N_t^k N_r)$ elements phased array setup, offering substantial performance gains with respect to the MIMO setup with linear reflectors.
Reflection models such as the one we consider here may be introduced into reflectors by means of various methods, depending on the specific application, e.g. by exploiting naturally occurring phenomena, or by introduction of active elements exhibiting desired nonlinear characteristics.

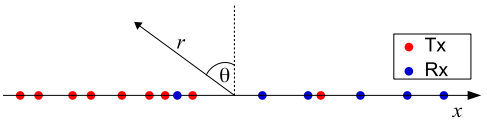

Fig. 1. Tx and Rx antenna arrays

2. PROPAGATION MODEL

Consider a far field scene distributed along the azimuthal and radial axes θ and r respectively. For convenience define $\psi \equiv \frac{1}{2}\sin\theta, \psi \in [-\frac{1}{2}, \frac{1}{2})$ and $\tau \equiv \frac{r}{c}$ where c is the propagation velocity, and parametrize the scene with (ψ, τ). A Tx antenna array illuminates the scene while an Rx array records the returns, as depicted in Fig. 1. The Tx and Rx arrays consist of N_t and N_r antennas, respectively, positioned at $\left\{x_0^t, \cdots, x_{N_t-1}^t\right\}$, $\left\{x_0^r, \cdots, x_{N_r-1}^r\right\}$.
The Tx transmits a narrow-band signal at frequency ω and wavelength $\lambda = \frac{2\pi c}{\omega}$. The complex envelope at the *n*th Tx antenna is $a_n(t)$ such that the resulting far field $E_i(\psi, \tau, t)$ is given by:

$$E_i(\psi, \tau, t) = \mathrm{Re}\left[\tilde{E}_i(\psi, \tau, t) e^{j\omega t}\right] \tag{1}$$

[*]This work was supported in part by NSF under Grant No. CCF-1319828, and AFOSR under Grant No. FA9550-11-1-0183.
[†]This work was supported in part by the ISF under Grant. No. 956/12.

where we have defined:

$$\tilde{E}_i(\psi,\tau,t) \equiv \sum_{n'=0}^{N_t-1} a_{n'}(t-\tau)\exp\left[j\frac{4\pi}{\lambda}x_{n'}^t\psi\right]e^{-j\omega\tau} \quad (2)$$

The scene is comprised of M point targets at a common distance τ_0 and azimuths $\psi_1,\cdots,\psi_M$. We consider a deterministic, *k*th power-law nonlinear reflection model such that the reflection generated at the *l*th target is:

$$E_r^l(\psi_l,\tau_0,t) = \beta_l\left(E_i(\psi_l,\tau_0,t)\right)^k \quad (3)$$

where β_l is the coupling strength of the *l*th target. In the sequel our estimation goal is the azimuths $\psi_1,\cdots,\psi_M$.
Next, develop expressions for the signal recorded at the Rx array. Using (1) and (3) we have for the complex envelope of the reflected signal component centred around $k\omega$:

$$\tilde{E}_r^l(\psi_l,\tau_0,t) = \beta_l\left(\sum_{n'=0}^{N_t-1} a_{n'}(t-\tau_0)\exp\left[j\frac{4\pi}{\lambda}x_{n'}^t\psi_l\right]\right)^k e^{-j\omega k\tau_0}$$

$$= \beta_l e^{-j\omega k\tau_0}\sum_{n''=0}^{N_t'-1}\hat{a}_{n''}(t-\tau_0)\exp\left[j\frac{4\pi}{\lambda}\hat{x}_{n''}^t\psi_l\right] \quad (4)$$

Where the second equation is retrieved from the first by application of the multinomial expansion, such that the sum over n'' is over $N_t' = \left(\binom{N_t}{k}\right) \equiv \binom{N_t+k-1}{k}$ unique (multinomial) solutions $\boldsymbol{\gamma}^{(n)} = [\gamma_0^{(n)},\gamma_1^{(n)},\cdots,\gamma_{N_t-1}^{(n)}]$ of the equation $\sum_{i=0}^{N_t-1}\gamma_i = k$, and the corresponding virtual Tx locations $\hat{x}_n^t$ and transmission functions $\hat{a}_n(t)$ are given according to:

$$\hat{a}_n(t) = \sqrt{c_n}\prod_{i=0}^{N_t-1} a_i^{\gamma_i^{(n)}}(t)$$

$$\hat{x}_n^t = \sum_{i=0}^{N_t-1}\gamma_i^{(n)}x_i^t$$

$$\sqrt{c_n} \equiv \binom{k}{\gamma_0^{(n)},\gamma_1^{(n)},\ldots,\gamma_{N_t-1}^{(n)}} \quad (5)$$

Notice that the nonlinear reflected signal as given in (4) is analogous to the reflected signal in a conventional setup with linear reflectors, virtual element positions $\hat{x}_n^t$ and signal set $\hat{a}_n(t)$.
The reflected signal propagates towards the Rx array with wavelength $\lambda_k = \frac{\lambda}{k}$ corresponding to the higher frequency. The received signal at the *m*th antenna element after down-converting to baseband is given according to:

$$\tilde{s}_m(t) = \sum_{l=1}^{M}\sum_{n''=0}^{N_t'-1}\hat{\beta}_l\hat{a}_{n''}(t-2\tau_0)\exp\left[j\frac{4\pi}{\lambda}\left(\hat{x}_{n''}^t+\hat{x}_m^r\right)\psi_l\right]e^{-j2\omega k\tau_0} \quad (6)$$

where $\hat{x}_m^r \equiv kx_m^r$ are the virtual Rx locations.

3. MAIN RESULT: DIRECTION OF ARRIVAL ESTIMATION

In this section we consider the DOA estimation problem in the presence of nonlinear reflectors and analyze the fundamental limits of target identifiability. We adapt the analysis of [1] for discrete-time MIMO radar configurations with linear reflectors to a continuous time formulation in conjunction with nonlinear reflectors and show that under ideal conditions it is possible to identify $O(N_t^k N_r)$ targets when utilizing the *k*th order nonlinearity, improving results derived for the linear case.
Define modified received signals as $\breve{s}_m(t) \equiv \tilde{s}_m(t+2\tau_0)e^{j2\omega k\tau_0}$. we have, using (6):

$$\breve{s}_m(t) = \sum_{n''=0}^{N_t'-1} c_{m,n''}(\boldsymbol{\beta},\boldsymbol{\psi})\hat{a}_{n''}(t) \quad (7)$$

where $c_{m,n''}(\boldsymbol{\beta},\boldsymbol{\psi}) \equiv \sum_{l=1}^{M}\beta_l\exp\left[j\frac{4\pi}{\lambda}\left(\hat{x}_{n''}^t+\hat{x}_m^r\right)\psi_l\right]$.
For the sequel define $C(\boldsymbol{\beta},\boldsymbol{\psi})$ to be a vector stacking the elements of $\{c_{m,n''}(\boldsymbol{\beta},\boldsymbol{\psi})\}$ in some arbitrary order.

Definition 3.1. *M targets are uniquely identifiable from $\{\breve{s}_m(t)\}$ if $\exists\{a_n(t)\}$ such that for every combination of not more than M targets we have that $\forall m : \breve{s}_m^1(t) = \breve{s}_m^2(t)$ implies $(\boldsymbol{\beta}_1,\boldsymbol{\psi}_1) = (\boldsymbol{\beta}_2,\boldsymbol{\psi}_2)$*

The problem of parameter identifiability is about determining the maximal number M of uniquely identifiable targets from $\{\breve{s}_m(t)\}$. Our main result for this section is the following one:

Theorem 3.1. *There exists a signaling set $\{a_n(t)\}$ and a selection of N_t Tx and N_r Rx antenna locations such that any $M < \frac{1}{2}\left(\lfloor\frac{N_t+k-1}{k}\rfloor^k N_r+1\right) = O(N_t^k N_r)$ targets are identifiable from $\{\breve{s}_m(t)\}$.*

We will prove a series of useful lemmas and end this section with the proof of theorem 3.1. First, start with a definition:

Definition 3.2. *We say that M targets are uniquely identifiable from $C(\boldsymbol{\beta},\boldsymbol{\psi})$ if for every combination of not more than M targets we have that $C(\boldsymbol{\beta}_1,\boldsymbol{\psi}_1) = C(\boldsymbol{\beta}_2,\boldsymbol{\psi}_2)$ implies $(\boldsymbol{\beta}_1,\boldsymbol{\psi}_1) = (\boldsymbol{\beta}_2,\boldsymbol{\psi}_2)$.*

The next lemma regarding the signal set design is used in proving subsequent claims:

Lemma 3.1. *There exists a set of N_t functions $\{a_n(t)\}$ such that the corresponding functions $\{\hat{a}_n(t)\}$, generated according to (5) hold: $\int_t\hat{a}_{n'}(t)\hat{a}_n^*(t)dt = \delta_{nn'}\hat{g}_n$, with $\hat{g}_n$ a constant.*

Proof. See section 5. □

The next lemma is a restatement of results in [5] with appropriate adaptations to continuous time:

Lemma 3.2. *A necessary condition for parameter identifiability from the received signals $\{\breve{s}_m(t)\}$ is parameter identifiability from $C(\boldsymbol{\beta},\boldsymbol{\psi})$. It is also sufficient if the signaling set satisfies lemma 3.1.*

Proof. Given $\{a_n(t)\}$ the $\{\breve{s}_m(t)\}$ are determined from the elements of $C(\boldsymbol{\beta},\boldsymbol{\psi})$ as per (7). We trivially have that if M parameters are not identifiable from $C(\boldsymbol{\beta},\boldsymbol{\psi})$ they are also not identifiable from $\{\breve{s}_m(t)\}$.
Conversely, assume that M targets are uniquely identifiable from $C(\boldsymbol{\beta},\boldsymbol{\psi})$ and that the signaling set satisfies lemma 3.1. We show that the target parameters are uniquely identifiable from $\{\breve{s}_m(t)\}$. Indeed, using (7) we have that the following holds at the receiver: $\int_t\breve{s}_m(t)\hat{a}_{n''}^*(t)dt = \hat{g}_{n''}c_{m,n''}(\boldsymbol{\beta},\boldsymbol{\psi})$. Repeating this for every m and n'' we can extract $C(\boldsymbol{\beta},\boldsymbol{\psi})$, and since it allows unique identification of the parameters so does $\{\breve{s}_m(t)\}$. □

Using lemma 3.2 we have that the number of identifiable targets from $\{\check{s}_m(t)\}$ is equal to the number of identifiable targets from $C(\boldsymbol{\beta},\boldsymbol{\psi})$. The next lemma is useful for the proof of the main theorem.

Lemma 3.3. *There exists a set of N_t Tx and N_r Rx antenna locations $\{x_n^t\},\{x_n^r\}$ such that the set $\{\hat{x}_{n''}^t+\hat{x}_m^r\}$ contains $N_s=\left\lfloor\frac{N_t+k-1}{k}\right\rfloor^k N_r=O(N_t^k N_r)$ contiguous points on a uniform $\frac{\lambda}{2}$-spaced grid (starting at 0 without loss of generality).*

Proof. See section 4. □

Finally, we can prove the main theorem:

Proof. (Theorem 3.1) For the sensor locations choose a setup that satisfies lemma 3.3 with $N_s=\left\lfloor\frac{N_t+k-1}{k}\right\rfloor^k N_r$ the number of contiguous samples $\{\hat{x}_{n''}^t+\hat{x}_m^r\}$. Define the vector $\tilde{C}(\boldsymbol{\beta},\boldsymbol{\psi})$ as a subvector of $C(\boldsymbol{\beta},\boldsymbol{\psi})$ according to:

$$\tilde{C}(\boldsymbol{\beta},\boldsymbol{\psi})\equiv\left[\sum_{l=1}^{M}\beta_l e^{j2\pi 0\psi_l},\cdots,\sum_{l=1}^{M}\beta_l e^{j2\pi(N_s-1)\psi_l}\right]^T \tag{8}$$

the number of identifiable targets from $\tilde{C}(\boldsymbol{\beta},\boldsymbol{\psi})$ is not greater than the number of identifiable targets from $C(\boldsymbol{\beta},\boldsymbol{\psi})$ as the former contains a subset of the elements of the latter. Given L targets define:

$$\begin{aligned}&\boldsymbol{B}(\boldsymbol{\psi})\equiv\left[B'(\psi_1),\cdots,B'(\psi_L)\right]\\&B'(\psi)\equiv[\exp(j2\pi 0\psi),\cdots,\exp(j2\pi(N_s-1)\psi)]^T\\&\boldsymbol{\beta}\equiv[\beta_1,\cdots,\beta_L]^T\end{aligned} \tag{9}$$

and notice that with these definitions we have $\tilde{C}(\boldsymbol{\beta},\boldsymbol{\psi})=\boldsymbol{B}(\boldsymbol{\psi})\boldsymbol{\beta}$. As any N_s distinct vectors $\{B'(\psi_1),\cdots,B'(\psi_{N_s})\}$ are linearly independent (stacked side by side they form a Vandermonde matrix), we use the result from [6], [7] (Thm. 1) to claim that a sufficient condition for parameter identifiability from $\tilde{C}(\boldsymbol{\beta},\boldsymbol{\psi})$ is $L<\frac{N_s+1}{2}$, such that plugging the expression for N_s we have that we can uniquely identify any $M<\frac{1}{2}\left(\left\lfloor\frac{N_t+k-1}{k}\right\rfloor^k N_r+1\right)=O(N_t^k N_r)$ point targets, which is our key result. □

4. ANTENNA ARRAY DESIGN

In this section we design antenna arrays in conjunction with lemma 3.3. The goal is to choose positions $\{x_n^t,x_n^r\}$ such that the resulting virtual positions $\{\hat{x}_n^t,\hat{x}_n^r\}$ satisfy the conditions of the lemma, with $\{\hat{x}_n^t+\hat{x}_m^r\}$ covering a contiguous uniform $\frac{\lambda}{2}$-spaced grid of $\left\lfloor\frac{N_t+k-1}{k}\right\rfloor^k N_r=O(N_t^k N_r)$ elements.

The virtual Tx antenna locations are determined from the physical antenna locations according to (5). Our construction will result in virtual arrays such that the virtual Tx array will span a uniform grid of spacing $N_r\frac{\lambda}{2}$ while the virtual Rx array will span a grid with spacing $\frac{\lambda}{2}$.

For the Rx array choose $\{x_n^r\}$ on a uniform grid with spacing $\frac{\lambda}{2k}$:

$$x_n^r=n\frac{\lambda}{2k}\qquad\qquad n=0,\cdots,N_r-1 \tag{10}$$

which, coupled with the definition $\hat{x}_m^r\equiv kx_m^r$ results in the desired virtual Rx array.

As for the Tx array, our design problem hints at the one studied in [8] where the authors considered the diversity of the co-array formed according to position differences between pairs of physical elements. They showed that a nested geometry maximizes the number of degrees of freedom available for DOA estimation with a given number of elements.

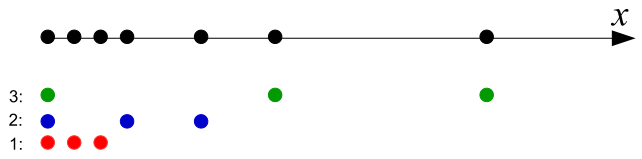

Fig. 2. A Tx array (black) and its three constituent hierarchies with three elements each. The first element is shared between hierarchies such that the overall number of elements is $N_t=7$.

For nonlinear imaging, virtual locations $\hat{x}_n^t$ are formed as k-sums of positions x_m^t. We use nested arrays similar to those proposed in [8] and obtain Tx diversity of $O(N_t^k)$ virtual elements covering a uniform $N_r\frac{\lambda}{2}$-spaced grid as required.

With *k*th order nonlinearity we design a nested Tx array partitioned into k hierarchies. The *i*th hierarchy is a uniformly spaced array with N_t^i elements and spacing d_t^i, such that all hierarchies share a common element at location 0. An example for $k=3$ is depicted in Fig. 2 with the three hierarchies in color and the resulting array in black. The first $i=1$ Tx hierarchy is designed with spacing $d_t^1=N_r\frac{\lambda}{2}$ and yet unspecified number of elements N_t^1. Subsequent hierarchies are designed according to the following iterative rule: For the *(i+1)*th Tx hierarchy choose spacing $d_t^{i+1}=N_t^i d_t^i$ and again, a yet unspecified number of elements N_t^i. For simplicity, taking into account the k multiplicity of the common 0 element, populate all hierarchies with an equal number of $N_t^i=\left\lfloor\frac{N_t+(k-1)}{k}\right\rfloor$ elements discarding the remaining antennas.

With this design, we show that the virtual Tx array covers an $\left\lfloor\frac{N_t+(k-1)}{k}\right\rfloor^k$ elements uniform contiguous grid with spacing $N_r\frac{\lambda}{2}$. Indeed, the virtual Tx array contains every k-sum of element positions. Specifically, it contains any such sum with exactly one element from each of the k hierarchies, and these result in unique virtual elements due to the geometric spacing of the sub-arrays. The overall number of such combinations equals $(N_t^i)^k=\left\lfloor\frac{N_t+(k-1)}{k}\right\rfloor^k$.

Combining with the N_r Rx elements we end up with $\{\hat{x}_n^t+\hat{x}_m^r\}$ covering a contiguous uniform $\frac{\lambda}{2}$-spaced grid of $\left\lfloor\frac{N_t+(k-1)}{k}\right\rfloor^k N_r$ elements.

5. SIGNAL SET SYNTHESIS

In this section we provide a proof for lemma 3.1. Namely, we design a signal set $\{a_n(t)\}$ such as to satisfy the correlation property $\int_t\hat{a}_{n'}(t)\hat{a}_n^*(t)dt=\delta_{nn'}\hat{g}_n$. In what follows we present a construction technique that results in constant modulus signals, which is desirable for practical applications.

For *k*th order nonlinearity and N_t transmitters the Tx signals $\{a_n(t)\},n=0,\cdots,N_t-1$ are defined to be windowed pure discrete tones amplitude modulating a rectangular shaping function:

$$a_n(t)=\sum_{m=0}^{\Omega_{N_t}-1}\exp(j2\pi\frac{\Omega_n m}{\Omega_{N_t}})h(t-mT_c) \tag{11}$$

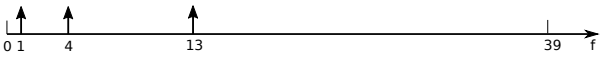

Fig. 3. Signal set frequency occupation for $k = 3$ nonlinearity and $N_t = 3$ transmitters: $\Omega_0 = 1, \Omega_1 = 4, \Omega_2 = 13$.

where $h(t) = \mathbb{1}_{0 \le t \le T_c}(t)$ is a rectangular shaping function and T_c the chip length. The nth discrete tone frequency Ω_n is defined recursively according to:

$$\begin{cases} \Omega_0 = 1 \\ \Omega_n = k\Omega_{n-1} + 1, \qquad n \ge 1 \end{cases} \tag{12}$$

The discrete tones are windowed to a finite time record of length Ω_{N_t}. This is schematically depicted in Fig. 3 for $k = 3$ and $N_t = 3$.

With the definition above and using (5), the virtual signal set becomes:

$$\hat{a}_{n'}(t) = \sqrt{c_{n'}} \sum_{m=0}^{\Omega_{N_t}-1} \exp(j2\pi \frac{m}{\Omega_{N_t}} \sum_{j=0}^{N_t-1} \gamma_j^{(n')} \Omega_j) h(t - mT_c) \tag{13}$$

We now show that the signal set as defined satisfies lemma 3.1. The next lemma is useful for proving the orthogonality relations:

Lemma 5.1. *for every* $\{\gamma_i \ge 0\}$*, such that* $\sum_{i=0}^{N_t-1} \gamma_i = k$*:*

1. $\sum_{i=0}^{R-1} \gamma_i \Omega_i < \Omega_R$ *for every* $R \le N_t$
2. $\{\gamma_i\}$ *are uniquely determined from* $u = \sum_{i=0}^{N_t-1} \gamma_i \Omega_n$

Proof. The first claim is easy. To prove the second claim, use the first claim with $R = N_t - 1$ to show $\gamma_{N_t-1} = \left\lfloor \frac{u}{\Omega_{N_t-1}} \right\rfloor$. Then, apply the same procedure on $u - \gamma_{N_t-1}\Omega_{N_t-1}$ get γ_{N_t-2} and continue similarly for all following coefficients. □

Finally, using $\int_t h(t - mT_c)h^*(t - mT_c) = T_c$ we have:

$$\int_t \hat{a}_{n'}(t)\hat{a}_n^*(t)dt =$$

$$T_c\sqrt{c_{n'}c_n} \sum_{m=0}^{\Omega_{N_t}-1} \exp(j2\pi \frac{m}{\Omega_{N_t}^k} \left[\sum_{j=0}^{N_t-1} \gamma_j^{(n')}\Omega_j^k - \sum_{j=0}^{N_t-1} \gamma_j^{(n)}\Omega_j^k \right]) =$$

$$\delta_{nn'}\hat{g}_n \tag{14}$$

with $\hat{g}_n = T_c c_n \Omega_{N_t}^k$, where in the last equality we have used lemma 5.1 to claim that the term in brackets is zero if and only if $n = n'$. Thus, our signal set adheres to lemma 3.1 as required.

6. NUMERICAL EXPERIMENT

We complement our analysis with the results of a numerical experiment. The setup is comprised of 13 far-field reflecting targets with angles as depicted in red in Fig. 4. The targets exhibit nonlinear reflectance with $k = 3$ and unit coupling coefficients $\beta = 1$. We design a Tx array with $N_t = 7$ elements according to the scheme of section 4 and the example given there as the union of three constituent equi-populated sub-arrays. In units of $\frac{\lambda}{2}$ the constituent sub-arrays are positioned at $\{0, 1, 2\}, \{0, 3, 6\}, \{0, 9, 18\}$ such that the Tx locations are $\{0, 1, 2, 3, 6, 9, 18\}$ as in Fig. 2. The receiver array is degenerate with a single element at $x_0^r = 0$. For the signaling set we implemented the design scheme of section 5 with tones

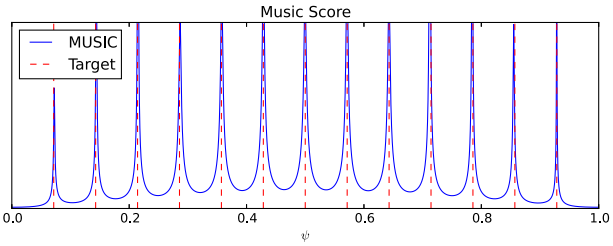

Fig. 4. Single-shot MUSIC score for 13 $k = 3$ nonlinear reflecting targets and a setup as described in the text.

$\Omega \in \{1, 4, 13, 40, 121, 364, 1093\}$ and a sequence length equal to $\Omega_7 = 3280$ chips. To probe the stability of the estimation problem we have included the effect of a complex AWGN impairing the received signal. For the simulation described here we have assumed SNR = 10dB. With the setup as defined above the virtual array strictly covers the contiguous section $\{0, \cdots, 26\}$ which was used in the estimation procedure.

For DOA estimation we implemented a single-shot MUSIC algorithm [9]. In Fig. 4 we plot the score function vs. ψ where it is evident that the algorithm gives excellent estimates for the location of all 13 targets, in accord with Theorem 3.1 which guarantees identifiability of up to 13 targets under these conditions. Also notice that with seven transmitting elements and one receiving element conventional MIMO radar techniques cannot support DOA estimation for more than 6 targets under any circumstances, such that the above experiment exemplifies the additional degrees of freedom supported by the nonlinear interaction between the probing field and the reflecting targets.

7. DISCUSSION

We have introduced the notion of target probing through nonlinearities as a means to enhance the number of identifiable targets in applications utilizing antenna arrays in MIMO configurations. We have shown that a virtual Tx array emerges in conjunction with the nonlinearities such that the effective number of degrees of freedom available for DOA estimation is asymptotically orders of magnitude larger than available in conjunction with linear reflectors.

Our result reveals an inherent asymmetry between the Tx and Rx arrays under such nonlinearities as is evident from our expression for the number of identifiable targets which scales as $O(N_t^k N_r)$. An effective way to reap the most benefit from the proposed scheme would be to introduce a single element for the Rx while transmitting with multiple antennas at the Tx, which would lead to the biggest impact under a constraint on the total number of antennas.

With respect to DOA estimation performance in noisy environments our nonlinear scheme inherits performance bounds from conventional results pertaining to DOA estimation with linear targets with corresponding virtual arrays and signal sets replacing physical ones. A full account of this will be provided in future work. We also leave the detailed analysis of the bandwidth expansion phenomenon coupled with the nonlinear interaction to future work.

A topic we have only briefly alluded to is the applicability of the nonlinear reflectors model to practical applications. Sophisticated probing-field-target interaction models have yet to be fully exploited by conventional radar systems. Further research is required to evaluate if such models can be implemented in practice.

8. REFERENCES

[1] J. Li and P. Stoica, "MIMO radar with colocated antennas," *IEEE Signal Processing Mag.*, vol. 24, no. 5, pp. 106–114, 2007.

[2] E. Fishler, A. Haimovich, R. S. Blum, L. J. Cimini, D. Chizhik, and R. A. Valenzuela, "Spatial diversity in radars-models and detection performance," *IEEE Trans. on Signal Process.*, vol. 54, no. 3, pp. 823–838, 2006.

[3] J. R. Lindner, "Microbubbles in medical imaging: current applications and future directions," *Nature Reviews Drug Discovery*, vol. 3, no. 6, pp. 527–533, 2004.

[4] J. Mertz, "Nonlinear microscopy: new techniques and applications," *Current opinion in neurobiology*, vol. 14, no. 5, pp. 610–616, 2004.

[5] J. Li, P. Stoica, L. Xu, and W. Roberts, "On parameter identifiability of MIMO radar," *IEEE Signal Process. Lett.*, vol. 14, no. 12, pp. 968–971, 2007.

[6] A. Nehorai, D. Starer, and P. Stoica, "Direction-of-arrival estimation in applications with multipath and few snapshots," *Circuits, Syst. and Signal Process.*, vol. 10, no. 3, pp. 327–342, 1991.

[7] M. Wax and I. Ziskind, "On unique localization of multiple sources by passive sensor arrays," *IEEE Trans. on Acoust., Speech and Signal Process.*, vol. 37, no. 7, pp. 996–1000, 1989.

[8] P. Pal and P. P. Vaidyanathan, "Nested arrays: a novel approach to array processing with enhanced degrees of freedom," *IEEE Trans. on Signal Process.*, vol. 58, no. 8, pp. 4167–4181, 2010.

[9] W. Liao and A. Fannjiang, "MUSIC for single-snapshot spectral estimation: Stability and super-resolution," *Applied and Computational Harmonic Analysis*, 2014.